



Development of Martian saline seep models and their implications for planetary protection

Madelyn K. Mettler^{a,b,1}, Hannah M. Goemann^{a,c,1}, Rebecca C. Mueller^{a,d}, Oscar A. Vanegas^e, Gabriela Lopez^f, Nitin Singh^g, Kasthuri Venkateswaran^g, Brent M. Peyton^{a,b,h,*}

^a Center for Biofilm Engineering, Montana State University, Bozeman, MT, USA

^b Department of Chemical and Biological Engineering, Montana State University, Bozeman, MT, USA

^c Department of Microbiology and Cell Biology, Montana State University, Bozeman, MT, USA

^d USDA Agricultural Research Service, Western Regional Research Center, Albany, CA, USA

^e University of Georgia, Athens, GA, USA

^f Georgia State University, Atlanta, GA, USA

^g NASA Jet Propulsion Laboratory, California Institute of Technology, Pasadena, CA, USA

^h Thermal Biology Institute, Montana State University, Bozeman, MT, USA

ARTICLE INFO

Keywords:

Biofilm
Mars
Halophile
Drip flow reactor
Next-generation sequencing

ABSTRACT

While life on Mars has not been found, Earth-based microorganisms may contaminate the Red Planet during rover expeditions and human exploration. Due to the survival advantages conferred by the biofilm morphology to microorganisms, such as resistance to UV and osmotic stress, biofilms are particularly concerning from a planetary protection perspective. Modeling and data from the NASA Phoenix mission indicate that temporary liquid water might exist on Mars in the form of high salinity brines. These brines could provide colonization opportunities for terrestrial microorganisms brought by spacecraft or humans. To begin testing for potential establishment of microbes, results are presented from a simplified laboratory model of a Martian saline seep inoculated with sediment from Hailstone Basin, a terrestrial saline seep in Montana (USA). The seep was modeled as a sand-packed drip flow reactor at room temperature fed media with either 1 M MgSO₄ or 1 M NaCl. Biofilms were established within the first sampling point of each experiment. Endpoint 16S rRNA gene community analysis showed significant selection of halophilic microorganisms by the media. Additionally, we detected 16S rRNA gene sequences highly similar to microorganisms previously detected in two spacecraft assembly cleanrooms. These experimental models provide an important foundation for identifying microbes that could hitchhike on spacecraft and may be able to colonize Martian saline seeps. Future model optimization will be vital to informing cleanroom sterilization procedures.

1. Introduction

Robotic space exploration is becoming increasingly attainable for government agencies and the private sector with the advancement of technology, especially regarding further exploration of Mars. Such advancements carry increased responsibility for planetary protection as outlined by the International Committee on Space Research's (COSPAR) Panel on Planetary Protection Policies [1,2]. The most current iteration of policies include strict guidelines on acceptable limits of bioburden on Martian rovers and other technical equipment, particularly in Mars Special Regions, regions deemed to have the most favorable conditions

for life to exist [3]. Achieving these levels of bioburden (for example, < 30 bacterial spores for equipment entering Special Regions of Mars) depends on contamination prevention in spacecraft assembly cleanrooms on Earth [3]. Despite the rigorous decontamination measures typically employed by cleanroom facilities [4,5], next-generation sequencing efforts have recently revealed the presence of non-culturable organisms frequently contaminating cleanrooms at higher levels than was previously thought possible [6–8]. These organisms are of particular concern for planetary protection as they potentially pose increased threats for forward contamination of Martian soils.

* Corresponding author. Center for Biofilm Engineering, Montana State University, Bozeman, MT, USA.

E-mail address: bpeyton@montana.edu (B.M. Peyton).

¹ These authors have contributed equally to this work.

The Martian landscape is notoriously hostile to life as we know it with its thin atmosphere, high levels of ultraviolet (UV) radiation, lack of pure liquid water, and low temperatures. Like Earth, Mars is highly heterogeneous with varying temperatures, topography, and soil composition throughout the planet. The temperatures on the surface of Mars average $-63\text{ }^{\circ}\text{C}$ compared to Earth's average of $13\text{ }^{\circ}\text{C}$ [9], although mathematical temperature modeling predicts surface temperatures in the lower latitudes can approach $22\text{ }^{\circ}\text{C}$ during a sunny summer sol [10, 11]. Water in the form of ice exists in many places on Mars, but negligible concentrations are present as water vapor in the atmosphere [12]. As thoroughly reviewed by Wray [13], the past decades have seen much debate on the presence of liquid water on Mars, with subsurface glacial lakes [14,15] and recurring slope lineae [16,17] receiving attention for their potential to host microbial life. It is largely agreed that the subsurface glacial reservoirs are likely stable high-salinity liquid brines existing at temperatures below the freezing point of pure water. However, whether the temporary recurring slope lineae are caused by dust or water is actively disputed [18,19]. Deliquescence with changes in seasonal relative humidity may also play an important role in the presence of briny liquids on Mars [13,20,21]. It is also possible that microenvironments habitable to life exist that are not accurately captured by the measurement devices used in exploration vehicles such as rovers and orbiters. Although concrete evidence for the ability for life to exist on Mars has yet to be revealed, these findings have sparked many questions regarding the possibility for terrestrial organisms brought by spacecraft to colonize Martian soil. As discussed by the COSPAR Panel on Planetary Protection, polyextremophilic biofilm-forming organisms are of high concern for planetary forward contamination [22].

Biofilms are microbial communities and are often surface-associated which provides many survival advantages over planktonic cells including increased resistance to antimicrobials, desiccation, and other environmental stresses such as UV radiation and osmotic lysis [23–29]. Biofilms pose a significant risk for planetary protection as they can contaminate spacecraft and subsequently the surfaces on which these spacecraft land. Recent experiments have shown that some polyextremophiles can survive for at least several months under Martian conditions [30,31]. Crisler et al. (2012) cultivated planktonic halophilic microorganisms under multiple Martian-relevant stressors (up to 2 M MgSO_4 and low pH) and through up to 15 freeze-thaw cycles until no viable organisms were able to be recovered [32]. However, given that biofilms confer increased tolerance to environmental stressors, there remains a wide knowledge gap in the ability of the biofilm morphology to enhance bacterial survival in Martian-relevant conditions.

Here we developed proof-of-concept experimental models which aim to 1) identify biofilm-forming halophiles on Earth that may survive in potential Martian briny liquid conditions and 2) determine whether any of these organisms overlap with those which have been detected in spacecraft assembly cleanrooms. The project utilized a simple Martian saline seep analog created using a drip flow biofilm reactor (DFR; Bio-Surface Technologies, Bozeman, MT) [33]. The DFR was inoculated with sediment from Hailstone Basin (HSB), a naturally occurring saline seep in south-central Montana. The high soil salinity is due to natural evaporation leading to the accumulation of salts (including sodium, magnesium, and sulfates) and heavy metals in the soil [34,35]. Additionally, as it is located in south-central Montana, the soil is exposed to freezing and subfreezing temperatures for much of the year, increasing its relevance to Martian conditions. To our knowledge, this research is the first microbiological study published about HSB. We used highly saline media to select for halophiles from the HSB, and used 16S rRNA-based microbial community sequencing from these experiments provide a guide for which microorganisms might survive the harsh Martian conditions. We then utilized publicly available datasets from cleanroom sampling efforts to identify overlap between the model communities and known cleanroom microbes. Comparing these microbes to those found in spacecraft assembly cleanrooms highlights possible taxa that could be of concern from a planetary protection perspective.

2. Methods

2.1. Inoculation material

The saline seep reactor was inoculated with sediment from HSB which was sampled in early June 2021 (coordinates: 46.00 N , -109.18 W ; Fig. 1). Additional sampling site details can be found in the Supplemental Information (Table S1) and in a U.S. Geological Survey report from 1979 [35]. Sediment was collected using sterile 50 mL conical vials and spatulas rinsed with 95% ethanol. After sampling, vials for DNA analysis were placed on dry ice for transit back to the laboratory and then transferred into a $-80\text{ }^{\circ}\text{C}$ freezer for storage and DNA extractions. Samples for DFR inoculation were kept on wet ice (approx. $4\text{ }^{\circ}\text{C}$) for transit to the laboratory.

2.2. Reactor setup and operation

The Martian seep analog used a DFR filled with sand with an average diameter of 2 mm (Fig. 2). The DFR is a well-characterized biofilm reactor with an American Society for Testing and Materials (ASTM) standard method for growing low-shear biofilms, but was modified for this study [33]. A small brass filter was placed interior to the effluent tubing to prevent sand from exiting the reactor through the effluent port. The reactor, including the filter, sand, and connected effluent tubing, was autoclaved for 20 min at $123\text{ }^{\circ}\text{C}$ and 21 psi prior to the experiments to ensure sterility. The silicone tubing for influent media was autoclaved separately and then attached to the reactor via sterile 23-gauge needles. Media was pumped into the system using peristaltic pumps operating at an average flow rate of 0.2 mL/min to each channel which was the lower limit of the pump's abilities. Two reactors (a total of ten channels) were used in the high-carbon experiments while only one reactor (a total of six channels) was used for the low-carbon experiments (Table 1). Six of the channels in the high-carbon experiments were under CO_2 conditions to closer mimic the Martian atmosphere compared the Earth's atmosphere (four channels), while all six channels for the low-carbon experiments were under CO_2 conditions [36]. A $0.2\text{ }\mu\text{m}$ air filter and the Tygon tubing for CO_2 were autoclaved prior to reactor assembly and inoculation. The DFR model was kept at room temperature to ensure the accumulation of an observable biofilm within the time constraints of the experiments. For both experiments, several internal channels were covered with foil and tape (Fig. 2) to block light from entering the reactor, mimicking subsurface light conditions. Approximately 5 g of HSB sediment was suspended via vortex mixing for at least 1 min in 40 mL of media in a sterile 50 mL conical vial to remove microorganisms from the sediment surface. After settling for 15–30 min when most of the particulates had fallen to the bottom of the vial, 7 mL of supernatant was used to inoculate each channel with the microbial community suspended in the respective media for each channel. The supernatant was pipetted over the entire length of each channel. Continuous flow of media was initiated approximately 24 h after the inoculation of the reactors. The DFR was left on a flat surface, allowing for slight pooling of media at the bottom of the channels.

2.3. Media

Three different media were used throughout the experiments. The initial high-carbon experiments used two different media: high-carbon MgSO_4 medium, which included 1 M MgSO_4 and 0.1 M NaCl, while the high-carbon NaCl medium featured 1 M NaCl and 0.1 M MgSO_4 . In both media, there was tryptone, KCl, glucose, and yeast extract based on the media used by Caton et al. (2004) to provide excess nutrients and promote rapid biofilm accumulation [37]. The low-carbon experiments used a third medium, low-carbon MgSO_4 that included 1 M MgSO_4 and 0.1 M NaCl but only yeast extract as the sole carbon source at 0.1% of the concentration used in the high carbon media. Media were prepared in 20 L carboys and autoclaved prior to use. Table 2 summarizes the

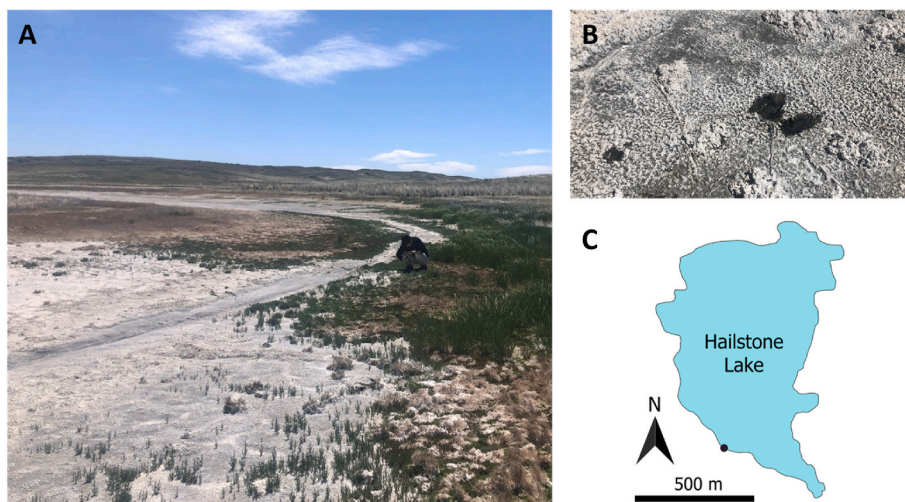


Fig. 1. A) Researcher examining a potential sampling location at Hailstone Basin near Rapelje, Montana. Samples were collected on the left side of the image where the soil has an upper white layer of salt. B) Close up image of sampled area. The dark spots mark where the upper salt layer was removed during collection. C) Map of the ephemeral Hailstone Lake with black dot marking the approximate sampling location.

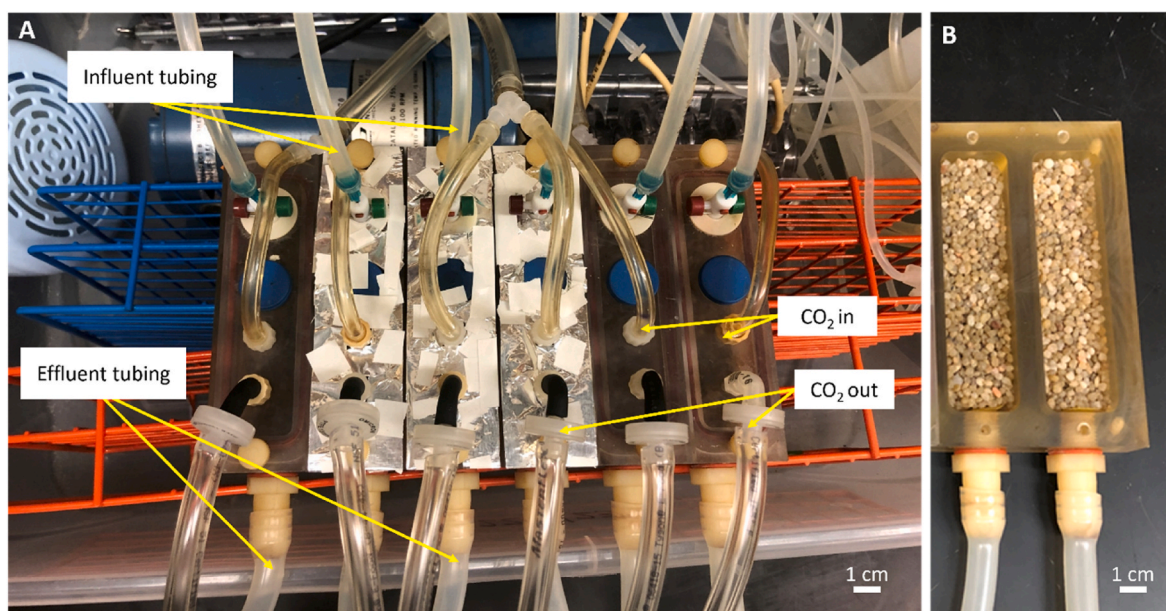


Fig. 2. A) Drip flow reactor set up at start of low-carbon experiment and B) sand in the reactor prior to start of experiment.

Table 1

Conditions for each channel for all experiments.

High-carbon experiment										
Channel	1	2	3	4	5	6	7	8	9	10
Medium	MgSO ₄	MgSO ₄	NaCl	NaCl	MgSO ₄	MgSO ₄	NaCl	NaCl	NaCl	NaCl
Light or dark	Light	Dark	Dark	Light	Light	Light	Dark	Dark	Light	Light
Under CO ₂	No	No	No	No	Yes	Yes	Yes	Yes	Yes	Yes
Low-carbon experiment										
Channel	1	2	3	4	5	6 ^a				
Medium	MgSO ₄									
Light or dark	Light	Dark	Dark	Light	Light	Light				
Under CO ₂	Yes	Yes	Yes	Yes	Yes	Yes				

^a Channel 6 in the low-carbon experiment served as an uninoculated control.

components of the media used in both experiments.

2.4. Sampling for culture-based measurements

For sampling, three grains of sand were removed from the surface layer of sand in each channel: one from the top (near the influent),

Table 2

Concentrations of components in the saline media.

	High-Carbon MgSO ₄ (g/L)	High-Carbon NaCl (g/L)	Low-Carbon MgSO ₄ (g/L)
MgSO ₄ ·7H ₂ O (epsomite)	246.5	58.4	246.5
NaCl	5.8	24.6	5.8
KCl	2.0	2.0	2.0
Yeast extract	1.0	1.0	0.001
Glucose	1.0	1.0	–
Tryptone	5.0	5.0	–

middle, and distal (near effluent) areas of the channels. Surface sand grains were not submerged in the pooled media at the bottom of the reactor. Sampled sand grains had fresh media flowing across the surface, so any microorganisms on the sand grains were likely to be attached biofilm. The sand was removed with flame-sterilized tweezers and placed into sterile 50 mL conical vials containing 10 mL of sterile 10% w/v NaCl. The biofilm on the sand grains was then disaggregated via an alternating series of 1 min vortex mixing and 1 min sonication, for a total of 5 min. Afterward, the disaggregated biofilm was filtered onto polycarbonate filters and stained for direct microscopy counts. The high-carbon experiments also included spread plating 100 µL of disaggregated biofilm on plates made with the respective media from the sampled channels with 7.5 g/L Gelrite. Spread plates were incubated on the benchtop at room temperature for two days prior to counting the colony forming units (CFU). No distinctions between morphologies were made in the colony counts.

Sanger sequencing was also conducted during the high-carbon experiments on colonies grown on GelRite plates collected from the reactor channels. DNA was extracted from individual colonies using the One-Tube Tissue DNA Extraction Kit (Bio Basic, Ontario, Canada), according to the manufacturer's instructions, but at one-tenth the volume recommended for colony extraction. The full-length 16S rRNA gene was amplified using the universal primers 27F (5'-AGAGTTT-GATCCTGGCTCAG-3') and 1492R (5'-GGTTACCTTGTACGACTT-3'). PCR condition details are provided in the supplemental information. Sequences with high quality forward and reverse sequences were merged using the online tool merger in the EMBOSS toolkit and sequences were classified using BLASTn. To determine if there was overlap between these culturable organisms and the ZOTUs identified via amplicon sequencing we used USEARCH to set the Sanger reads as a database against our full set of amplicon ZOTUs including the DFR models, JPL and TAS sequences (described in section 2.6 below). Any reads that matched to the Sanger database at 97% identity and had e-values less than 1e-06 were counted as positive hits.

2.5. Microscopy

Prior to imaging, cells from the disaggregated biofilms were stained with 25x SybrGold nucleic acid gel stain as initially described by Chen et al. (2001) with an increased incubation time and higher final stain concentration [38]. In short, the stain was prepared and mixed with the sample at a final concentration of 4x and allowed to incubate in the dark for 15 min. After incubation, stained cells were vacuum filtered onto 0.2 µm black polycarbonate filters which were then affixed to glass microscope slides for counting. A Nikon Eclipse E800 epifluorescent microscope with a green fluorescein isothiocyanate (FITC) filter was used to view and count the cells. Field emission scanning electron microscopy (FE SEM) was performed on several samples using a Zeiss Supra 55VP FE SEM. For FE SEM imaging, sand grains were removed from the reactor directly, placed in a sterile petri dish, and allowed to air dry in a biosafety cabinet. The sand grains were then gently poured on Ted Pella carbon tape and placed in the FE SEM for imaging.

2.6. Culture-independent DNA sequencing analysis

To determine the composition and diversity of sediment microbial communities in the original sediment collected from HSB, and the cultured biofilms, we performed 16S rRNA gene amplicon sequencing. For the biofilm samples, DNA was extracted directly from surface sand grains harvested from the reactor using flame-sterilized tweezers. Genomic DNA was extracted from 0.5 g samples using the Fast DNA SPIN Kit for soil (MP Biomedicals, Santa Ana, CA), according to the manufacturer's instructions. The analysis targeted the V4 region of the 16S rRNA gene using 515F-A (GTGYCAGCMGCCGCGGTAA) and 806R-B (GGACTACVSGGGTATCTAAT) primers from the Earth Microbiome Project with adapters for Illumina-based sequencing on the MiSeq platform. PCR reaction and sequencing preparation details are provided in the supplemental information. To compare the DFR biofilm communities to organisms detected in spacecraft assembly clean rooms, we cross-referenced the microorganisms detected in the DFR biofilms with those detected via metabarcoding of the 16S rRNA gene in two studies of spacecraft-assembly cleanroom sampling [7,39]. Sequences were downloaded from NCBI Bioprojects PRJEB15908 (8 samples) and PRJEB8763 (13 samples) from a cleanroom facility at Thales Alenia Space (TAS, European Space Agency) in Turin, Italy, and the Jet Propulsion Laboratory (JPL, NASA) in Pasadena, CA, USA. The JPL samples were partitioned into two treatment groups, one for total (T) community members detected in the JPL cleanrooms and one for samples treated with propidium monoazide (PMA) to capture only living cells.

Sequenced reads (paired-end 300 bp) were merged and combined with the TAS and JPL datasets. The combined sequences were then trimmed, quality filtered, and dereplicated with USEARCH. Zero-radius operational taxonomic units (ZOTUs) were identified with UNOISE3 (v.11.0.667, [40]). The 16S ZOTUs were classified using SINTAX against a modified version of the Genome Taxonomy Database (GTDB v. 202, [41]) where the number of sequences were reduced to one representative for each species with additional outgroup for mitochondria and chloroplast 16S sequences added to eliminate eukaryotic sequences. Community composition was assessed using R Statistical Software (v.4.1.2; [42]). Phylogenetic and taxonomic metrics were computed with the *phyloseq* and *vegan* packages [43,44] and relative abundances of ZOTUs were calculated with the *microbiome* package [45]. PERMANOVA was used to determine statistical effects in Bray-Curtis community dissimilarities [44]. Due to large differences in sequencing depth between the publicly available data and the DFR model libraries, ordination and community overlap was performed on the full dataset rarefied to 2079 reads per sample, while the DFR model sequences were separately rarefied to 24843 reads per sample for comparisons between the high-carbon and low-carbon experiments. A reference phylogeny was constructed using full length and near full length sequences of isolates and metagenome assemblies downloaded from GenBank. Reference sequences were aligned using mafft [46], and a maximum likelihood tree was constructed using RAxML with the GTR + gamma model [47]. Environmental sequences were then mapped onto the reference tree using pplacer [48] with reference-aligned sequences. The phylogenetic tree was then visualized and annotated using iTOL [49]. The overlap of taxa between datasets was determined using vennDiagram in the *MicEco* package in R-Studio [50].

3. Results

3.1. Biofilm accumulation

Biofilm growth and accumulation was detected in both the high-carbon and low-carbon experiments. The high-carbon experiments included both direct microscopy counts and heterotrophic plate counts (Fig. 3A, S1). The plate counts were about one order of magnitude lower than the direct counts for each treatment. The general trend for each experiment was a gradual increase in biofilm accumulation. According

to plate counts, the high-carbon experiments reached steady state with biofilm density of 7–9.5 \log_{10} CFU/cm² around 17 days after the start of continuous flow. The microscopy counts show steady state (biofilm density of 8–9 \log_{10} cells/cm²) was achieved by 10 days after the start of continuous flow, which was the first sampling point. On average, the channels receiving normal atmospheric air (channels 1–4) had more biofilm accumulation by the end of the experiments compared to the channels receiving pure CO₂ (channels 5–10). The low-carbon experiments using low-carbon MgSO₄ medium showed a one to two orders of magnitude reduction in direct cell counts compared to the high-carbon experiment using high-carbon MgSO₄ medium with an endpoint biofilm density of 5–8.5 \log_{10} cells/cm² (Fig. 3B). Once again, the general trend was slightly increased biofilm density across all channels over time. The uninoculated control channel initially fostered some cells, but after 34 days of flow, cell density dropped near the detection limit, settling at or below 2 \log_{10} cells/cm².

The biofilms in the low-carbon experiments took 20 days after the start of continuous flow to reach steady state according to direct cell counts. Channel 4 fostered the most biofilm accumulation by the end of the experiment peaking at 8.2 \log_{10} cells/cm² which is similar in density to the biofilm in the high-carbon experiment using high-carbon MgSO₄ medium and CO₂ conditions (channels 5 and 6, 8.1 and 7.4 \log_{10} cells/cm² respectively). As with the high-carbon experiments, in the low-carbon experiments there was no observed influence of light exposure on biofilm density between channels.

3.2. FE SEM imaging

Fig. 4 A and B show the sand grains before inoculation and after biofilm accumulation. The FE SEM images of the high-carbon experiment (Fig. 4C) revealed several morphologies within the sample. The topography of the sand grain can be seen as well as coccoidal and rod-shaped cells of varying sizes. Additionally, there is visible extracellular polymeric substances (EPS) blanketing the cells and the sand grain surface (Fig. 4B) further verifying successful biofilm formation.

3.3. Microbial community analysis

The final dataset including the samples from the high-carbon and low-carbon experiments, the two cleanrooms [7,39], and the original sediment from HSB contained 1052 ZOTUs. Bray-Curtis ordination of the community dissimilarities indicated strong separation among the five sub-datasets (Fig. 5, pseudoF = 5.35, R² = 0.552, p < 0.001). Within the model experiments, community composition differences were driven primarily by the high-carbon vs. low-carbon media (pseudoF = 4.8, R² = 0.423, p = 0.001, Fig. 5, Table S3), while we did not detect significant community effects of CO₂ vs. ambient air or light vs. dark conditions.

The HSB sediment used to inoculate the DFR consisted of 281 detected ZOTUs representing 25 distinct phyla of which the major phyla included the archaeal *Bacteroidota* (24%), and bacterial *Halobacteriota* (22%), *Proteobacteria* (18.4%, classes *Gammaproteobacteria* 96%,

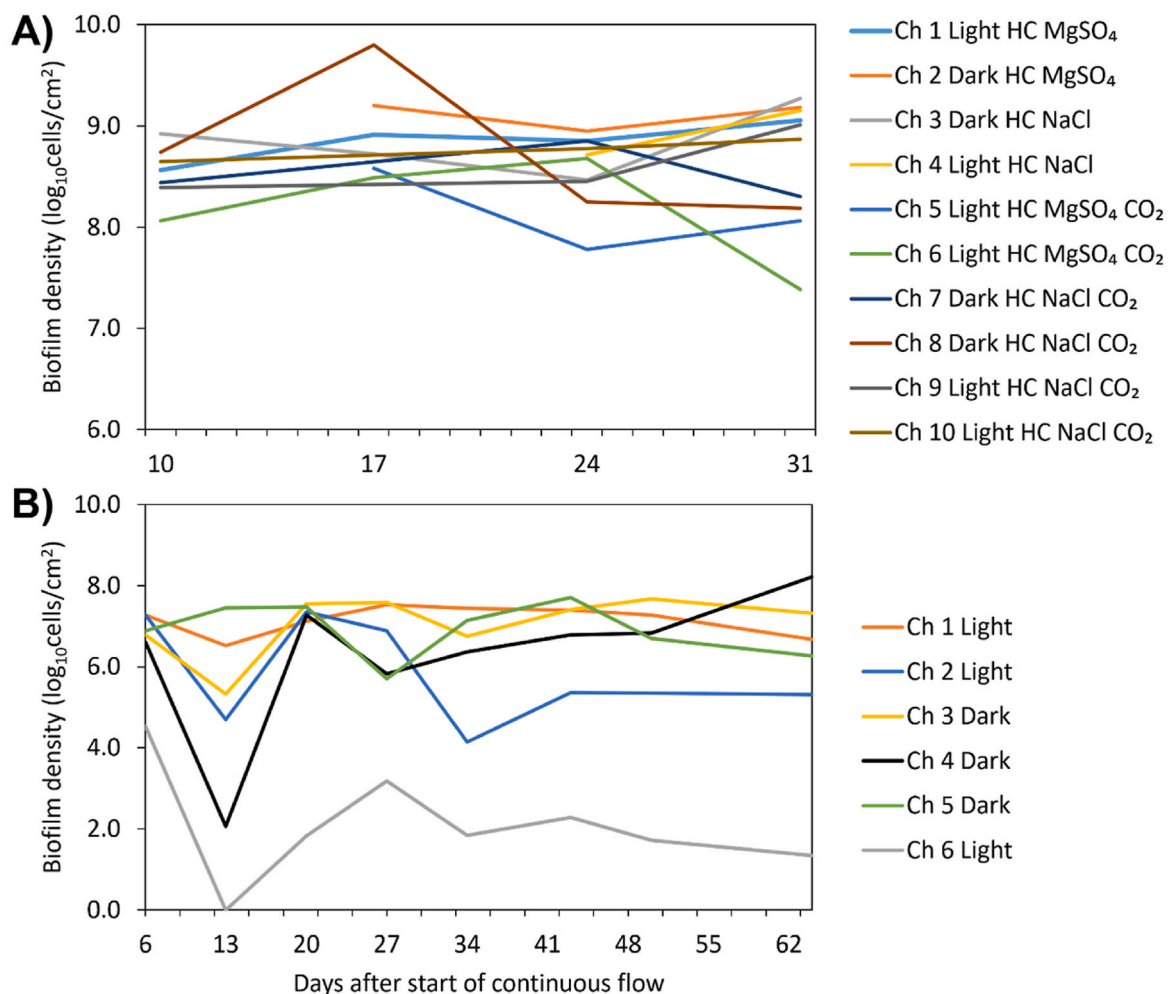


Fig. 3. Biofilm density of A) high-carbon experiment (HC) and B) low-carbon experiment (LC) as measured by epifluorescent microscopy direct counts. All channels in low-carbon experiment were fed MgSO₄ medium and CO₂. Note the different axes for each experiment.

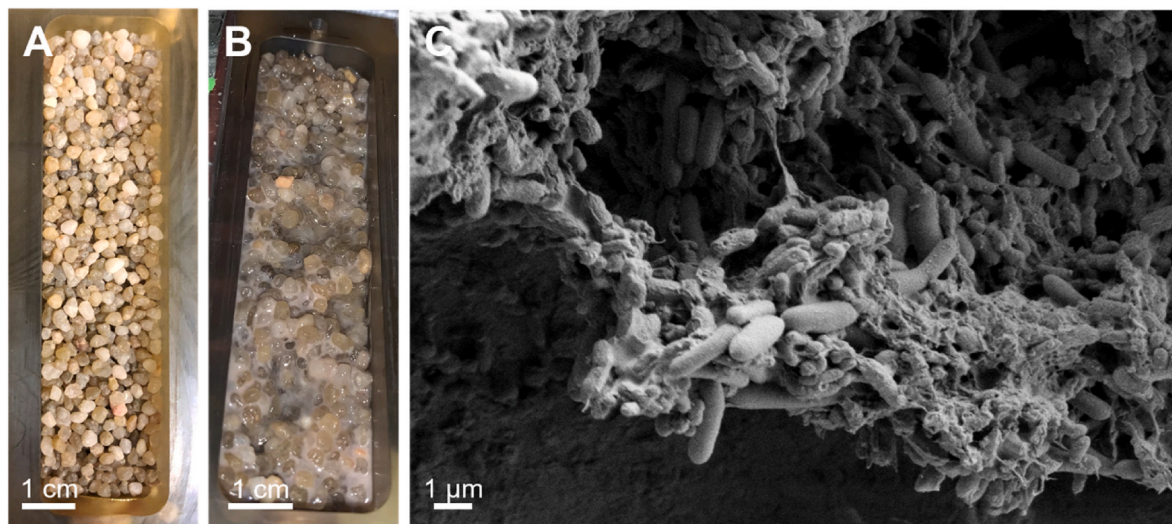


Fig. 4. A) Sand grains prior to sterilization and inoculation. B) Visible accumulation of biofilm on sand grains in channel 8 of high-carbon experiment. C) FE SEM image of biofilm attached to sand grain from panel B.

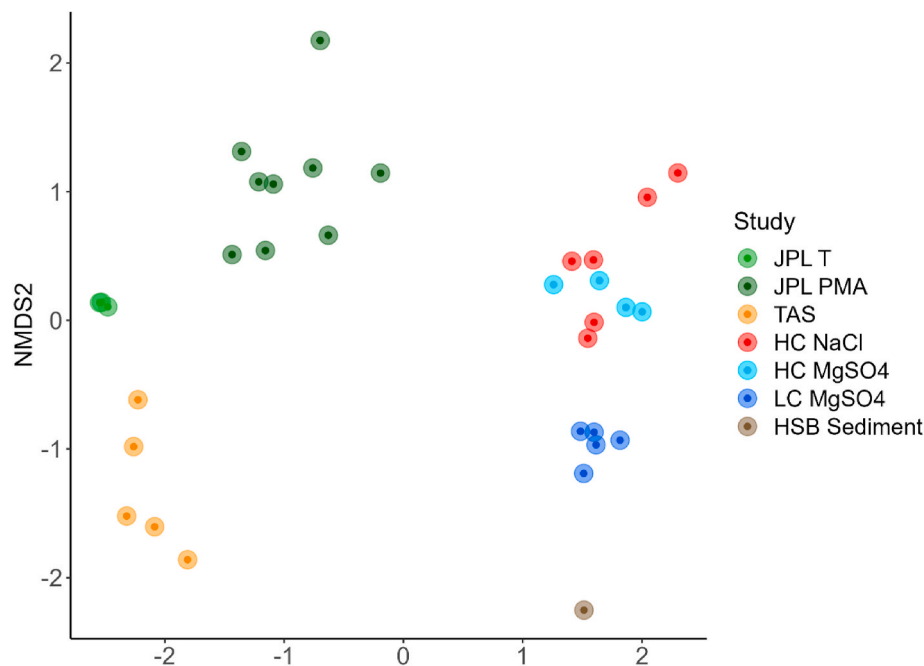


Fig. 5. Non-metric multi-dimensional scaling (NMDS) analysis using Bray-Curtis dissimilarities comparing the two cleanrooms (JPL and TAS), saline seep models, and HSB sediment. The JPL samples are differentiated by total community (JPL T) and PMA-treated (JPL PMA) and the DFR models are separated by their respective media (high-carbon = HC, low-carbon = LC).

Alphaproteobacteria 4%), *Firmicutes* (14.4%), *Desulfobacterota* (4.8%), *Chloroflexota* (4.2%), *Deinococcota* (3.2%), *Caldatibacteriota* (1.8%), and *Actinobacteria* (2.3%, Table S2). In the high-carbon experiment, the biofilm community consisted of 365 ZOTUs representing 9 distinct phyla dominated by *Gammaproteobacteria*, *Bacilli*, *Clostridia*, *Alphaproteobacteria*, and *Actinomycetia* classes (Fig. 6A). In the low-carbon experiments, we detected 404 ZOTUs representing 22 phyla, similarly dominated by *Gammaproteobacteria*, *Bacilli*, and *Actinomycetia* classes. Notably, in the low-carbon experiments the genus *Halomonas* (*Gammaproteobacteria*) accounted for $56 \pm 1.8\%$ of the community on average, compared to $26 \pm 0.66\%$ in the high-carbon experiments (Fig. 6B). In the high-carbon experiments additional comparisons were made between the media (dominant MgSO₄ or NaCl) with the main differences between the two media being greater presence of genera *Pseudidiomarina* and *Microbulifer*

in high-carbon MgSO₄ medium (Fig. 6B).

Cultured members of the DFR biofilm communities were identified by submitting full-length 16S Sanger sequencing to NCBI BlastN. Of the 24 colonies submitted for sequencing, nine were identified as *Pseudalteromonas* sp., eight were *Halomonas* sp., four were *Yersinia* sp., two were *Bacillus* sp. and one *Serratia* sp. (Table 3). Thirteen of these cultured organisms had matches at or above 97% identity amongst the uncultured 16S amplicon sequences. The Sanger read MP3.2 identified as a *Halomonas* sp. was most closely related to *H. alkaliphila*, and ZOTUs 1 and 2 (*H. titanicae*, *H. alkaliphila*, or *H. meridiana*) matched with 100% identity although Zotu1 had one single nucleotide polymorphism (SNP) between its 253 nt read and the 937 nt Sanger sequence. ZOTU 132 was also identified as a match to MP3.2 at 97% identity and was identified as *H. salifodinae*. An additional 16 ZOTUs matched with 97% identity to

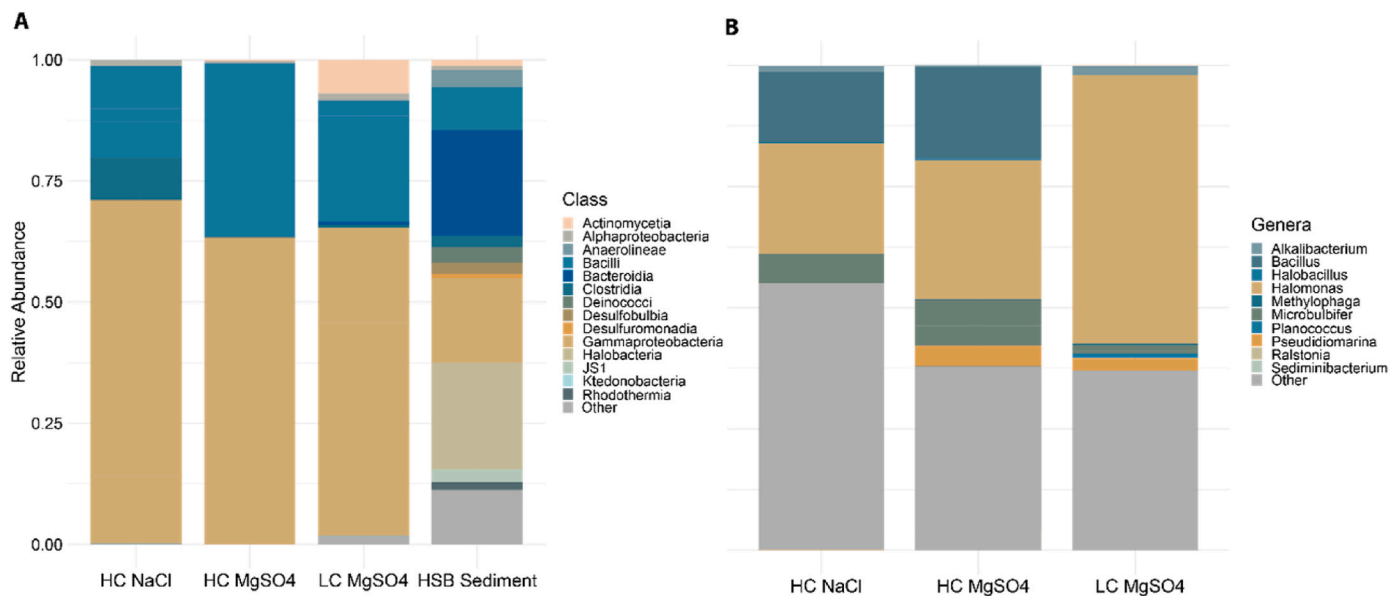


Fig. 6. Relative abundance of **A**) the 14 highest relative abundance classes across the high-carbon experiment (HC), low-carbon experiment (LC) and Hailstone Basin soil (HSB). **B**) The 10 highest relative abundance genera present in each of the three media tested in the DFR.

Sanger sample MP2.1 and were primarily identified as either *H. arcis* or *H. gomseomensis*. Zotu3 (*Bacillus subtilis* or *Bacillus atrophaeus*) matched with 100% identity to MP1.2 with an additional 17 ZOTUs matching to MP1.2 at 97–99.6% identity and most likely belonged to *B. subtilis* or *Metabacillus halosaccharovorans*. Three ZOTUs (7, 9 and 17) matched to MP3.1 (*Pseudoalteromonas translucida*). Lastly, seven ZOTUs matched to MP5.2_merged (*Serratia rubidaea*) at 97.2–100% identity and while three were likely *Serratia* sp., the other four were identified as *Escherichia coli*, *Lonsdalea quercina*, *Franconibacter daqui*, and *Pantoea vagans*. Sanger reads 10.3, 10.5, 3.1, 5.1, 8.2, 9.1, and 9.2 also matched to various ZOTUs belonging to *Halomonas* sp., *Pseudoalteromonas* sp. and *Yersinia* sp. but were not matched across the full length of the V4 region (App. 1).

Visualization of the ZOTUs in a phylogenetic tree confirmed the compositional trends of the model communities and indicated the presence of overlapping ZOTUs between the models and the cleanroom datasets (Fig. 7). The 16S Sanger sequences were also mapped to the tree and confirmed the BLASTn analysis of their likely taxonomies as *Halomonas* sp., *Pseudoalteromonas* sp., *Bacillus* sp. and several *Yersinia* sp. (Table S4). Venn diagram analysis of the models vs. the cleanroom ZOTUs confirmed the overlap of five ZOTUs between the original HSB sediment, the two DFR models, and the two cleanroom datasets (Fig. S8A) which were classified in Fig. S8B as *Halomonas titanicae*, *Actinotalea* sp., *Ralstonia solanacearum*, *Paracoccus marinus*, and *Preistia endophyticus*. Interestingly, an additional five ZOTUs were found to overlap between the models and both cleanrooms that were not found in the HSB sediment which included *Bacillus subtilis*, *Staphylococcus aureus*, *Cutibacterium acnes*, *Micrococcus aloeverae*, and *Rhodococcus qingshengii*. Additional shared taxa between the datasets are summarized in Appendix 2.

4. Discussion

4.1. Biofilm accumulation indicates a promising reactor design

Drip flow reactors were designed to grow low-shear biofilms and are often used for modeling medical and wound biofilms [78,79]. To our knowledge this study is the first to utilize a DFR to model Martian terrestrial conditions, an important first step in adapting this technology for astrobiological efforts. The DFR allows for long residence times,

flexibility with channel-to-channel treatments, and containment of substrate to model Martian regolith seeps. We used a simple, proof-of-concept experiment design to eliminate confounding factors such as the influence of substratum on biofilm formation that would occur using a more complicated regolith simulant. The model was kept at room temperature as temperatures up to 22 °C are found on the surface of Mars during a summer sol [10,11]. The high-carbon experiment was designed as a baseline for model development to compare several aspects that are strong drivers of microbial growth without being carbon-limited to confirm biofilm formation. Biofilm density of the high-carbon experiments was above 9.5 log₁₀ cells/cm² for several channels at various time points and biofilms were visible on the sand grains to the naked eye (Fig. 4B). As expected, microscopy counts were higher than the plate counts, since not all organisms are culturable on Gelrite plates. Further, plates were incubated at ambient laboratory conditions (exposed to O₂), so it is likely that the microorganisms cultured on plates were only a subset of the biofilm present in the channels under CO₂.

Once biofilm formation was confirmed with the high-carbon experiment, the low-carbon medium was designed to provide carbon at a level more comparable to known Martian regolith. In 2022, it was reported that Curiosity rover detected organic carbon in concentrations as high as 730 µg C/g [51]. In both experiments, the reactor media were designed to mimic possible chemical conditions of Martian saline seeps. Sulfates such as magnesium sulfate, including hydrated forms, specifically epsomite, have been detected on Mars which could lead to the formation of dense brines [52–54]. Additionally, potassium ions have been detected via remote sensing on Mars, and potassium chloride has been used in other laboratory models of Martian salts [55,56]. MgSO₄-dominated and NaCl-dominated media were compared due to the chaotic nature of high levels of Mg²⁺ ions which we expected to be more challenging to microbial growth [57]. Regardless of media formulation, each of the DFR biofilms achieved high steady state densities quickly after the start of continuous flow.

4.2. Halophiles dominate the DFR model biofilms

Culturing conditions strongly influenced biofilm community composition, with the communities separating by high-carbon or low-carbon and dominant medium salt. All DFR model biofilms were

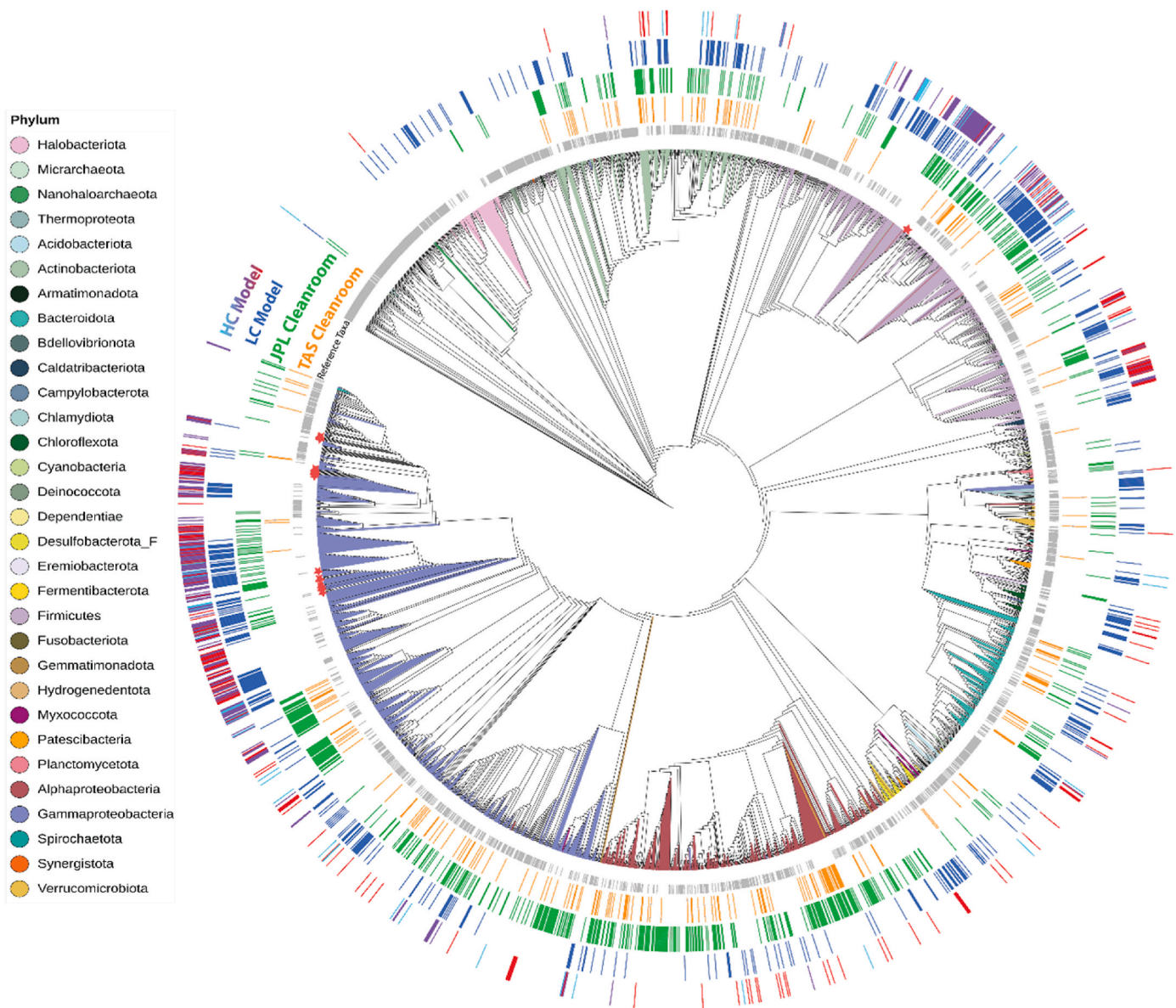


Fig. 7. Phylogenetic tree of cleanroom and model seep taxa. Colored strips represent ZOTUs present in each dataset. From inner to outer ring: Reference tree taxa, TAS cleanroom, JPL cleanroom, low-carbon model seep, high-carbon model seep. The high-carbon model is further separated by taxa present in only the NaCl-dominated medium (light blue), $MgSO_4$ -dominated medium (bright red) or both (purple). Culturable organisms identified by Sanger sequencing from biofilm colonies in the high-carbon experiment are indicated by stars (red) at branch ends. (For interpretation of the references to colour in this figure legend, the reader is referred to the Web version of this article.)

dominated by *Halomonas* sp. with additional matches to *Pseudoalteromonas* sp.. *Halomonas* sp. are almost uniformly halophilic and are known for producing sulfate-rich exopolysaccharides which may also explain their robust growth in the $MgSO_4$ -dominated media [58]. Several likely species of *Halomonas* were detected including the highly halotolerant *H. titanicae*, *H. alkaliphila*, and *H. meridiana* [59,60] although identification at the species levels is challenging due to the high level of conservation in the V4 region of the 16S rRNA gene beyond the genus level [61]. Furthermore, the presence of several possible *Halomonas* sp. among the culturable DFR biofilm community members identified by Sanger sequencing confirms the ability of members of this genus to grow in the variety of conditions related to a Martian saline seep environment tested here. The genus *Pseudoalteromonas* also consists of several halotolerant psychrophiles including *P. haloplanktis* which is considered a model cold-adapted bacterium [62]. Three ZOTUs from the DFR models were identified as matches to the Sanger read 3.1 (*Pseudoalteromonas translucida*) although they were more closely identified as

P. haloplanktis, *P. shioyasakiensis*, and *P. pyrdzensis*. *P. haloplanktis*, originally isolated from Antarctic seawater, has been a focal species for understanding microbial adaptation to cold temperatures and is a known biofilm producer [63].

Bacillus subtilis was the most common *Bacillus* species detected in the DFR biofilms, especially in the high-carbon experiment. Many strains of *B. subtilis* are halotolerant and capable of forming endospores [64] which could facilitate their survival in cleanrooms and onto spacecraft until potentially more favorable conditions are encountered in Martian saline seeps. Resuscitation of *B. subtilis* endospores can be largely prevented by Martian levels of UV radiation [65,66]. However, minimal coverage by Martian regolith is highly protective of UV radiation thus potentially allowing for resuscitation [67]. We detected *B. subtilis* among both the amplicon (total) and Sanger (culturable) DFR biofilm communities, confirming its robust growth across conditions and culturability after exposure to our hypothetical Martian conditions.

4.3. Implications for planetary protection

To prevent microbial contamination, spacecraft are assembled in cleanrooms which are facilities with strict air quality standards maintained via control of airborne particles, temperature, and humidity [68]. There are varying classes of cleanrooms which are defined by the number of airborne particulates present. The International Standards Organization (ISO) sets cleanroom standards to which both the National Aeronautics and Space Administration (NASA) and the European Space Agency (ESA) adhere [4–6]. Particulates are controlled with high efficiency particulate air (HEPA) filters, sticky mats, and suits that users are required to wear. Even with such measures in place, particulates, including microorganisms, persist in cleanrooms [6–8]. Cleaning and disinfecting procedures differ between organizations resulting in varying microbial communities between cleanrooms. Further, cleaning procedures of spacecraft hardware vary between organizations as discussed by Venkateswaran et al. and can include the use of 70% isopropanol wipes (NASA) or multiple-solvent cleaning (JPL) [69].

Having verified the successful cultivation of biofilm within the DFR under various conditions, we then determined whether there was overlap between the DFR biofilm communities and taxa that have been detected in spacecraft assembly cleanrooms. Halophiles *Halomonas titanicae* and *Planococcus marinus* were found to overlap between the DFR models and the cleanroom datasets. Importantly, *H. titanicae* was identified in both the PMA-treated (viable) and total community of JPL samples, and was detected in both the total and culturable communities of the DFR biofilms (Fig. 7). This suggests that not only is *H. titanicae* capable of contaminating and remaining viable in cleanrooms, but also has significant potential for survival in Martian brines. *B. subtilis* was also found to overlap between the models and the cleanrooms although it was not detected in the original HSB sediment. The failure to form biofilm or successfully sequence the uninoculated DFR control channel suggests that these organisms were likely truly present within the reactor conditions and not introduced via contamination during the sequencing process. Due to the low biomass of organisms in cleanrooms and subsequent low sequencing depth, there are likely additional undiscovered taxa in cleanrooms.

Together this evidence suggests a need for preventative measures against halophiles and endospore-formers in preparation for space flight as (i) they have previously been detected in cleanrooms suggesting they may have high potential for spacecraft contamination and, (ii) they have potential for proliferation in Martian seep conditions. Many of the overlapping taxa found in both the cleanrooms and the DFR experiments are unlikely to survive the Martian conditions not tested in the DFR, namely low temperatures and UV radiation. However, the presence of *B. subtilis* and additional *Bacillus* spore-formers provide potential forward contamination routes. Further, the lower temperature limit for *H. titanicae* is 4 °C for consistent growth which is within the known Martian temperature range [10,11,70,71]. *H. titanicae* resistance to UV radiation is unknown, however, the biofilm morphology can exhibit greater tolerance to UV radiation and other environmental stresses than individual cells of the same species [72]. While these organisms are not guaranteed to survive space travel, let alone the conditions found on Mars, these models can help inform cleanroom sterilization processes by illuminating the microorganisms of most significant concern. Further improvement of the models will provide even more accurate information for targeted cleanroom procedures. Additional methods for the disinfection and elimination of halophiles in cleanrooms must be developed. For the time being, methods from hide and fish curing/preservation including exposure to alternating electrical currents, ozone, and other chemistries could be employed [73–75]. These methods likely require alteration to comply with cleanroom practices and spacecraft hardware.

4.4. Improvements for future models

Now that the concept of biofilm formation in the modified DFR with non-standard microbial communities has been demonstrated, the model can be improved by incorporation of more relevant Martian conditions. Though Martian regolith has varying compositions, a laboratory simulant should be employed with a more defined chemistry, specifically including iron. Further, our initial model experiments were conducted at room temperature, representing the upper end of the surface temperatures found on Mars. For greater accuracy, future experiments should take place in a refrigerator or freezer, with cyclic temperature changes. Such changes would likely select for psychrophilic halophiles which are hypothesized to be the most capable of survival in Martian conditions. The DFR biofilms were exposed to either ambient atmosphere or fed pure CO₂ while the Martian atmosphere is composed of 96% CO₂ with Ar and N₂ being the next most abundant at about 2% each and other trace components [36]. The inclusion of Ar and N₂, as well as the use of tubing not permeable to oxygen would increase relevance to the Martian atmosphere. Additionally, there was no UV stress included in these experiments. Perhaps one of the greatest barriers for terrestrial life proliferating on Mars is the high flux of UVB and UVC, often considered entirely sterilizing for Earth microorganisms [76]. Though the pores of the regolith could offer some protection from such radiation [77], including UV dosage in future experiments would create a more powerful and realistic model.

Future experiments should also carefully consider the methods of inoculation and reactor sampling. While we thoroughly vortexed the inoculum prior to inoculation, it is possible that some organisms remained attached to sediment particles and were not inoculated into the reactor. We also detected several taxa in the DFR biofilms that did not overlap with the original HSB sediment. These community members could have been present below the level of detection in HSB sediment or could have been introduced to the reactor during sampling as the reactor was not placed in a biosafety cabinet. We also suggest including an expanded library of terrestrial inoculum and/or targeted studies of specific taxa.

5. Conclusions

Parallel experiments using a high-carbon Martian saline seep analog were completed to confirm feasibility of the reactor system and growth of HSB organisms in the DFR. Subsequent experiments with a low-carbon saline seep analog containing media with low carbon availability similar to that detected on Mars were completed. Biofilm accumulation occurred in all three media tested and biofilms reached steady state densities within several weeks of starting the experiments. The medium composition was the greatest driver of the resulting biofilm community composition. Light and atmospheric conditions were not observed to affect community composition. Additionally, several taxa were present in the reactor experiments that have been detected by sequencing in spacecraft assembly clean rooms. Microbes in or on spacecraft (built in assembly clean rooms) have the potential to contribute to forward contamination. The overlap between cleanroom and DFR biofilm taxa represents microorganisms that should inform cleanroom sterilization practice targets to prevent the transmission of microbes that may be capable of Martian saline seep colonization. In addition, future improvements of these models may help inform COSPAR policies on planetary protection to ensure responsible space exploration.

Funding

This research was supported by the National Science Foundation Research Experience for Undergraduates program (#2050856) and a fellowship from the Montana Space Grant Consortium.

CRedit authorship contribution statement

Madelyn K. Mettler: conducted experimental design, was a primary manuscript author, carried out the experiments and data analysis. **Hannah M. Goemann:** was a primary manuscript author, carried out the bioinformatics data analysis. **Rebecca C. Mueller:** carried out the experiments and data analysis. **Oscar A. Vanegas:** conducted experimental design; carried out the experiments and data analysis. **Gabriela Lopez:** conducted experimental design; carried out the experiments and data analysis. **Brent M. Peyton:** conducted experimental design, carried out the experiments and data analysis; all authors contributed to editing and revising the manuscript. **Nitin Singh:** contributed to conceptual plan for early data analysis and to editing and revising the manuscript. **Kasturi Venkateswaran:** contributed to conceptual plan for early data analysis and to editing and revising the manuscript.

Declaration of competing interest

The authors declare the following financial interests/personal relationships which may be considered as potential competing interests: Madelyn Mettler reports financial support was provided by Montana Space Grant Consortium. Gabriela Lopez reports financial support was provided by National Science Foundation. Oscar Vanegas reports financial support was provided by National Science Foundation.

Data availability

Data will be made available on request.

Acknowledgments

We would like to thank the US Fish and Wildlife Service for allowing us to sample at Hailstone National Wildlife Refuge (permit #21-006).

Appendix A. Supplementary data

Supplementary data to this article can be found online at <https://doi.org/10.1016/j.biofilm.2023.100127>.

References

- [1] COSPAR. COSPAR policy on planetary protection. 2021.
- [2] Coustenis A, Kminek G, Hedman N. The COSPAR panel on planetary protection. 2021. p. 2232.
- [3] Rummel JD. Special regions in Mars exploration: problems and potential. *Acta Astronaut* 2009;64(11):1293–7.
- [4] International Standards Organization. Cleanrooms and associated controlled environments — Part 1: classification of air cleanliness by particle concentration. 2015.
- [5] International Standards Organization. Cleanrooms and associated controlled environments — Part 2: monitoring to provide evidence of cleanroom performance related to air cleanliness by particle concentration. 2015.
- [6] Moissl-Eichinger C. Extremophiles in spacecraft assembly clean rooms. In: Stan-Lotter H, Fendrihan S, editors. *Adaption of microbial life to environmental extremes: novel research results and application*. Vienna: Springer Vienna; 2012. p. 231–61.
- [7] Mahnert A, et al. Cleanroom maintenance significantly reduces abundance but not diversity of indoor microbiomes. *PLoS One* 2015;10(8):e0134848.
- [8] Hendrickson R, et al. Clean room microbiome complexity impacts planetary protection bioburden. *Microbiome* 2021;9(1):238.
- [9] Williams DR. NASA Mars fact sheet. 2021 December 23. Available from: <https://nssdc.gsfc.nasa.gov/planetary/factsheet/marsfact.html>; 2021.
- [10] Pajola M, et al. Geology, in-situ resource-identification and engineering analysis of the vernal crater area (Arabia Terra): a suitable Mars human landing site candidate. *Planet Space Sci* 2022;213:105444.
- [11] Spanovich N, et al. Surface and near-surface atmospheric temperatures for the Mars Exploration Rover landing sites. *Icarus* 2006;180(2):314–20.
- [12] Smith MD, et al. The climatology of carbon monoxide and water vapor on Mars as observed by CRISM and modeled by the GEM-Mars general circulation model. *Icarus* 2018;301:117–31.
- [13] Wray JJ. Contemporary liquid water on mars? *Annu Rev Earth Planet Sci* 2021;49(1):141–71.
- [14] Lauro SE, et al. Multiple subglacial water bodies below the south pole of Mars unveiled by new MARSIS data. *Nat Astron* 2021;5(1):63–70.
- [15] Orosei R, et al. Radar evidence of subglacial liquid water on Mars. *Science* 2018; 361(6401):490–3.
- [16] Chevrier VF, Rivera-Valentin EG. Formation of recurring slope lineae by liquid brines on present-day Mars. *Geophys Res Lett* 2012;39(21).
- [17] Stillman DE. Chapter 2 - unraveling the mysteries of recurring slope lineae. In: Soare RJ, Conway SJ, Clifford SM, editors. *Dynamic Mars*. Elsevier; 2018. p. 51–85.
- [18] McEwen AS, et al. Mars: abundant recurring slope lineae (RSL) following the planet-encircling dust event (PEDE) of 2018. *J Geophys Res: Planets* 2021;126(4): e2020JE006575.
- [19] McEwen AS, et al. Seasonal flows on warm martian slopes. *Science* 2011;333(6043):740.
- [20] Möhlmann D, Thomsen K. Properties of cryobrines on mars. *Icarus* 2011;212(1): 123–30.
- [21] Abotalib AZ, Heggy E. A deep groundwater origin for recurring slope lineae on Mars. *Nat Geosci* 2019;12(4):235–41.
- [22] Rettberg P, et al. Planetary protection and mars special regions—a suggestion for updating the definition. *Astrobiology* 2016;16(2):119–25.
- [23] Flemming H-C, Neu TR, Wozniak DJ. The EPS matrix: the “House of biofilm cells”. *J Bacteriol* 2007;189(22):7945–7.
- [24] Donlan RM. Biofilms: microbial life on surfaces. *Emerg Infect Dis* 2002;8(9): 881–90.
- [25] Esbelin J, Santos T, Hébraud M. Desiccation: an environmental and food industry stress that bacteria commonly face. *Food Microbiol* 2018;69:82–8.
- [26] Roberson EB, Firestone MK. Relationship between desiccation and exopolysaccharide production in a soil *Pseudomonas* sp. *Appl Environ Microbiol* 1992;58(4):1284–91.
- [27] Mah T-FC, O’Toole GA. Mechanisms of biofilm resistance to antimicrobial agents. *Trends Microbiol* 2001;9(1):34–9.
- [28] Yin W, et al. Biofilms: the microbial “protective clothing” in extreme environments. *Int J Mol Sci* 2019;20(14).
- [29] Elasm MO, Miller RV. Study of the response of a biofilm bacterial community to UV radiation. *Appl Environ Microbiol* 1999;65(5):2025–31.
- [30] Beblo-Vranesevic K, et al. Surviving Mars: new insights into the persistence of facultative anaerobic microbes from analogue sites. *Int J Astrobiol* 2022;21(2): 110–27.
- [31] Volger R, et al. Mining moon & mars with microbes: biological approaches to extract iron from Lunar and Martian regolith. *Planet Space Sci* 2020;184:104850.
- [32] Crisler JD, et al. Bacterial growth at the high concentrations of magnesium sulfate found in Martian soils. *Astrobiology* 2012;12(2):98–106.
- [33] International A. Astm e2647-20: standard test method for quantification of *Pseudomonas aeruginosa* biofilm grown using drip flow biofilm reactor with low shear and continuous flow. 2020.
- [34] Miller MR, et al. Saline seep development and control in the north American great plains - hydrogeological aspects. *Agric Water Manag* 1981;4(1):115–41.
- [35] Lewis BD, Custer SG, Miller MR. Saline-seep development in the Hailstone Basin, northern stillwater county, Montana. In: *Water-resources investigations report; 1979* [Reston, VA].
- [36] Mahaffy PR, et al. Abundance and isotopic composition of gases in the martian atmosphere from the curiosity rover. *Science* 2013;341(6143):263–6.
- [37] Caton TM, et al. Halotolerant aerobic heterotrophic bacteria from the great salt plains of Oklahoma. *Microb Ecol* 2004;48(4):449–62.
- [38] Chen F, et al. Application of digital image analysis and flow cytometry to enumerate marine viruses stained with SYBR gold. *Appl Environ Microbiol* 2001; 67(2):539–45.
- [39] Koskinen K, et al. Microbial biodiversity assessment of the European Space Agency’s ExoMars 2016 mission. *Microbiome* 2017;5(1):143.
- [40] Edgar RC. UNOISE2: improved error-correction for Illumina 16S and ITS amplicon sequencing. *bioRxiv*; 2016.
- [41] Parks DH, et al. GTDB: an ongoing census of bacterial and archaeal diversity through a phylogenetically consistent, rank normalized and complete genome-based taxonomy. *Nucleic Acids Res* 2022;50(D1):D785–94.
- [42] R Core Team R. A language and environment for statistical computing. Vienna, Austria: R Foundation for Statistical Computing; 2021.
- [43] McMurdie PJ, Holmes S. phyloseq: an R package for reproducible interactive analysis and graphics of microbiome census data. *PLoS One* 2013;8(4):e61217.
- [44] Oksanen J, Kindt R, Simpson GL. *The vegan Package*. 2009.
- [45] Lahti L, Shetty S. Tools for microbiome analysis in R. e. al.. 2017.
- [46] Katoh K, Standley DM. MAFFT multiple sequence alignment software version 7: improvements in performance and usability. *Mol Biol Evol* 2013;30(4):772–80.
- [47] Stamatakis A. RAxML-VI-HPC: maximum likelihood-based phylogenetic analyses with thousands of taxa and mixed models. *Bioinformatics* 2006;22(21):2688–90.
- [48] Matsen FA, Kodner RB, Armbrust EV, pplacer. Linear time maximum-likelihood and Bayesian phylogenetic placement of sequences onto a fixed reference tree. *BMC Bioinf* 2010;11(1):538.
- [49] Letunic I, Bork P. Interactive Tree of Life (iTOL) v5: an online tool for phylogenetic tree display and annotation. *Nucleic Acids Res* 2021;49(W1):W293–6.
- [50] Russel J. MicEco: various functions for microbial community data. 2022.
- [51] Stern JC, et al. Organic carbon concentrations in 3.5-billion-year-old lacustrine mudstones of Mars. *Proc Natl Acad Sci USA* 2022;119(27):e2201139119.
- [52] Visscher AM, et al. Growth performance and root transcriptome remodeling of *Arabidopsis* in response to Mars-like levels of magnesium sulfate. *PLoS One* 2010;5(8):e12348.

- [53] Sheppard RY, et al. Updated perspectives and hypotheses on the mineralogy of lower Mt. Sharp, Mars, as seen from orbit. *J Geophys Res: Planets* 2021;126(2): e2020JE006372.
- [54] Bristow TF, et al. Brine-driven destruction of clay minerals in Gale crater, Mars. *Science* 2021;373(6551):198–204.
- [55] Nuding DL, et al. The aqueous stability of a Mars salt analog: instant Mars. *J Geophys Res: Planets* 2015;120(3):588–98.
- [56] Hecht MH, et al. Detection of perchlorate and the soluble chemistry of martian soil at the Phoenix lander site. *Science* 2009;325(5936):64–7.
- [57] Seckbach J, Oren A, Stan-Lotter H. *Polyextremophiles: life under multiple forms of stress*, vol. 27. Springer; 2013.
- [58] Bejar V, et al. Characterization of exopolysaccharides produced by 19 halophilic strains of the species *Halomonas eurihalina*. *J Biotechnol* 1998;61:135–41.
- [59] Romano I, et al. *Halomonas alkaliphila* sp. nov., a novel halotolerant alkaliphilic bacterium isolated from a salt pool in Campania (Italy). *J Gen Appl Microbiol* 2006;52(6):339–48.
- [60] Tourova TP, et al. Genomic and physiological characterization of halophilic bacteria of the genera *Halomonas* and *marinobacter* from petroleum reservoirs. *Microbiology* 2022;91(3):235–48.
- [61] Rossi-Tamisier M, et al. Cautionary tale of using 16S rRNA gene sequence similarity values in identification of human-associated bacterial species. *Int J Syst Evol Microbiol* 2015;65(Pt 6):1929–34.
- [62] Parrilli E, et al. The art of adapting to extreme environments: the model system *Pseudoalteromonas*. *Phys Life Rev* 2021;36:137–61.
- [63] Médigue C, et al. Coping with cold: the genome of the versatile marine Antarctica bacterium *Pseudoalteromonas haloplanktis* TAC125. *Genome Res* 2005;15(10): 1325–35.
- [64] Errington J, Aart LTV. Microbe Profile: *Bacillus subtilis*: model organism for cellular development, and industrial workhorse. *Microbiology (Read)* 2020;166(5): 425–7.
- [65] Schuerger AC, et al. Survival of endospores of *Bacillus subtilis* on spacecraft surfaces under simulated martian environments: implications for the forward contamination of Mars. *Icarus* 2003;165(2):253–76.
- [66] Osman S, et al. Effect of shadowing on survival of bacteria under conditions simulating the Martian atmosphere and UV radiation. *Appl Environ Microbiol* 2008;74(4):959–70.
- [67] Mancinelli RL, Klovstad M. Martian soil and UV radiation: microbial viability assessment on spacecraft surfaces. *Planet Space Sci* 2000;48(11):1093–7.
- [68] Whyte W. *Cleanroom technology: fundamentals of design, testing and operation*. John Wiley & Sons; 2010.
- [69] Venkateswaran K, et al. Evaluation of various cleaning methods to remove *Bacillus* spores from spacecraft hardware materials. *Astrobiology* 2004;4(3):377–90.
- [70] Valero A, et al. Modelling the growth boundaries of *Staphylococcus aureus*: effect of temperature, pH and water activity. *Int J Food Microbiol* 2009;133(1–2): 186–94.
- [71] Sánchez-Porro C, et al. *Halomonas titanicae* sp. nov., a halophilic bacterium isolated from the RMS Titanic. *Int J Syst Evol Microbiol* 2010;60(Pt 12):2768–74.
- [72] de Carvalho C. Biofilms: microbial strategies for surviving UV exposure. *Adv Exp Med Biol* 2017;996:233–9.
- [73] Hussain SA, Sarker MI, Yosief HO. Efficacy of alkyltrimethylammonium bromide for decontaminating salt-cured hides from the red heat causing moderately halophilic bacteria. *Lett Appl Microbiol* 2020;70(3):159–64.
- [74] Birbir Y, et al. Annihilation of extremely halophilic archaea in hide preservation salt using alternating electric current. *Johnson Matthey Technol Rev* 2015;59(2): 109–19.
- [75] Stevens DA, et al. *Halomonas*, a newly recognized human pathogen causing infections and contamination in a dialysis center: three new species. *Medicine* 2009;88(4):244–9.
- [76] Cockell CS, et al. The ultraviolet environment of Mars: biological implications past, present, and future. *Icarus* 2000;146(2):343–59.
- [77] Hallsworth JE. Mars' surface is not universally biocidal. *Environ Microbiol* 2021; 23(7):3345–50.
- [78] Manner S, Goeres D, Skogman M, et al. Prevention of *Staphylococcus aureus* biofilm formation by antibiotics in 96-Microtiter Well Plates and Drip Flow Reactors: critical factors influencing outcomes. *Sci Rep* 2017;7:43854. <https://doi.org/10.1038/srep43854>.
- [79] Woods J, Boegli L, Kirker KR, Agostinho AM, Durch AM, deLancey Pulcini E, et al. Development and application of a polymicrobial, in vitro, wound biofilm model. *J Appl Microbiol* 2012;112(5):998–1006. <https://doi.org/10.1111/j.1365-2672.2012.05264.x>.